

Scaling in a cellular automaton model of earthquake faults

M. Anghel,^{†±} W. Klein,^{†±}, J. B. Rundle,^{‡*} and J. S. Sá Martins^{*}

[†]Center for Nonlinear Studies, LANL, Los Alamos, NM 87545

[‡]Physics Department, University of Colorado at Boulder, Boulder, CO 80309

^{*}Colorado Center for Chaos and Complexity, CIRES, University of Colorado at Boulder, Boulder, CO 80309

[±]Permanent address: Physics Department and Center for Computational Science, Boston University, Boston, MA 02215

We present theoretical arguments and simulation data indicating that the scaling of earthquake events in models of faults with long-range stress transfer is composed of at least three distinct regions. These regions correspond to three classes of earthquakes with different underlying physical mechanisms. In addition to the events that exhibit scaling, there are larger “breakout” events that are not on the scaling plot. We discuss the interpretation of these events as fluctuations in the vicinity of a spinodal critical point.

Earthquake faults and fault systems are known to exhibit scaling [1,2] where the number N_M of earthquakes with seismic moment M scales as $N_M \sim 1/M^B$ with B between 1.5 and 2.0 [2]. The observed scaling is over several decades, but for the larger events there is an indication that scaling does not apply, a fact often attributed to poor statistics. However, because models also produce this deviation from scaling, even when there are many large events [4,5], the origin of this deviation lies elsewhere. Other questions of interest include: What is the physical mechanism that produces the scaling? Do all the events on the scaling plots have the same physical origin? We report the results of our theoretical and numerical investigations of a cellular automaton (CA) model of an earthquake fault indicating that the scaling region is dominated by a spinodal-like (pseudospinodal) singularity that determines the distribution of events. The scaling can be decomposed into three distinct regions driven by different physical mechanisms. In addition to the scaling region, we find that the largest “earthquakes” are not on the scaling plot and have yet another physical origin.

The system of interest is a CA version of the slider block model [3] and consists of a discrete two-dimensional ($d = 2$) array of blocks connected by linear springs with a spring constant (stress Green’s function) $T(r_{ij})$ and to a loader plate by linear springs with constant K_L ; r_{ij} is the distance between blocks. Each block i initially receives a random position U_i from a uniform distribution, and the loader plate contribution to the stress is set to 0. The stress σ_i on each block is given by $\sigma_i(t) = \sum_j T(r_{ij})[U_j(t) - U_i(t)] + K_L[V \sum_n \Theta(n-t) - U_i(t)]$ and compared to a threshold value σ_i^F . If $\sigma_i < \sigma_i^F$, the block is not moved. If $\sigma_i \geq \sigma_i^F$, the block slips (fails) and is moved according to $U_i(t+1) = U_i(t) + [\sigma_i(t) - \sigma_i^R(t)]/K$, where $K = K_L + K_C$, and $K_C = \sum_{j, i \neq j} T(r_{ij})$. The residual stress, $\sigma_i^R(t) = \sigma^R + a(\eta_i(t) - 0.5)$, specifies the stress on a block immediately after failure. The random noise η_i is taken from a uniform distribution between 0 and 1, a sets the noise amplitude, and σ^R is the average residual stress. After all the blocks have been tested and

moved, the stress on each block is measured again and the process is repeated. We choose $T_{ij} = K_C/q$ for all j inside a square interaction range with area $(2R+1)^2$ centered on site i , where $q = (2R+1)^2 - 1$ is the number of neighbors; $T_{ij} = 0$ for all the sites outside the interaction range. After block i slips, K_C/K of the local stress drop, $\sigma_i - \sigma_i^R$, is distributed equally to its neighbors, and K_L/K is dissipated. When no block has a stress greater than σ_i^F , the earthquake ceases and the seismic moment released during the event is $M = \sum_i \Delta U_i$, where ΔU_i is the slip of block i during the earthquake. The loader plate is then moved a distance $V\Delta T$, the stresses are updated, and we search for the unstable blocks that will initiate the next event. The quantity ΔT , which we set equal to 1, sets the “tectonic” time scale. In the limit $V = 0$ the stress is globally incremented to bring the “weakest” block to failure and there is a single initiator per plate update.

Because the T_{ij} appropriate for earthquake faults is long-range [5], we will consider $R \gg 1$. In our simulations $R = 30$, $\sigma_i^F = \sigma^F = 1$ is a spatial constant, $K_L = 1$, $K_C = 100$, $V = 0$, and the distribution of residual stresses is defined by $\sigma^R = 0.25$ and $a = 0.5$. In Fig. 1 we plot the log (base 10) of the probability $n(s)$ of events of size s (number of failing blocks) versus $\log(s)$ generated by the model. For the chosen parameters there are no multiple failures of the same block during an earthquake and $M \sim s$. For the total of 18×10^6 events, there is still a significant spread of the data in the large events region. The origin of this spread is not poor statistics.

We now review the theoretical arguments that describe the scaling of events. In the limit that R diverges such that $\int r^2 T(r) d\vec{r} \rightarrow \infty$ but $\int T(r) d\vec{r}$ is finite, we have derived a Langevin equation for the stress [5,6]. This derivation and numerical simulations [5,7] confirm that the CA model is described by equilibrium statistical mechanics in the limit of $R \rightarrow \infty$ and that this description is a very good approximation for systems with long, but not infinite, R . Because this Langevin equation is a general description of systems with a simple scalar order param-

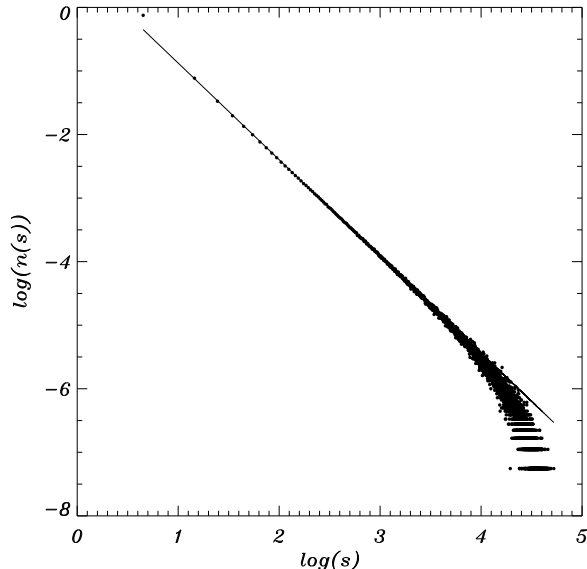


FIG. 1. Log-log plot of the probability $n(s)$, the number of events with s failing blocks divided by their total number, 18×10^6 . The system consists of 256×256 blocks with periodic boundary conditions. Note the deviation from the straight line of slope 1.5 ± 0.05 for large s .

eter [8], the scaling of the fluctuations in the vicinity of spinodals of mean-field Ising models (and simple fluids) and the present CA model is the same.

Our main assumption is that the structure and dynamics of earthquake events is identical to the structure and dynamics of fluctuations near critical points and spinodals. In particular, scaling is determined by the presence of a spinodal singularity [5,6]. For Ising systems, by mapping the thermal critical point onto a properly chosen percolation model [9,10], the properties of the fluctuations at the thermal critical point can be obtained from the properties of the clusters at the percolation threshold: percolation clusters are the physical realization of the fluctuations [9,10]. At the critical point the clusters associated with the divergent connectedness length are the fluctuations associated with the divergent susceptibility in the thermal model. We can use a similar mapping to generate a percolation model for the spinodal. Therefore, we can describe the scaling of events in the CA model in the language of cluster scaling for Ising models.

We first discuss how the cluster structure relates to thermal critical phenomena in non-mean-field systems ($R = 1$) where hyperscaling is valid. In this case, the mean number of clusters in a region of volume ξ^d , where ξ is the correlation length, is one. In such systems the critical phenomena fluctuation in this volume is isomorphic to the cluster [9]. This picture is altered in mean-field systems. For mean-field Ising systems ($R \rightarrow \infty$)

there is a line of spinodal critical points in addition to the usual critical point. These mean-field thermal singularities can also be mapped onto percolation transitions [10], but the relation between percolation clusters and critical fluctuations is qualitatively different. The mean number of clusters in a volume ξ^d is $N_c = R^d \epsilon^{2-d/2}$ near the critical point and $N_s = R^d \Delta h^{3/2-d/4}$ near the spinodal [11–14]. Here $\epsilon = (T - T_c)/T_c$, where T_c is the critical temperature, and $\Delta h = h - h_s$, where h_s is the value of the magnetic field at the spinodal for a fixed temperature $T < T_c$. The factor R^d appears because all lengths are in units of the interaction range. The Ginsburg criterion for mean-field critical points is $\epsilon^{-\gamma}/(R^d \epsilon^{2\beta-d\nu}) \ll 1$ [8]. That is, the system is well approximated by mean-field theory if the fluctuations are small compared to the order parameter. Using the mean-field exponents [8] $\gamma = 1$, $\beta = 1/2$ and $\nu = 1/2$, the Ginsburg criterion is equivalent to $N_c \gg 1$. We will refer to systems with $N_c \gg 1$ but finite as near-mean-field. A similar argument is used near the spinodal to show that $N_s \gg 1$ for near-mean-field.

Because $N_c \gg 1$, the meaning of order parameter scaling is changed. For systems with hyperscaling [8], the density of the single cluster with diameter ξ scales as ϵ^β , as does the order parameter. In mean-field and near-mean-field systems, ϵ^β cannot be the density of a single cluster, because that would lead to a magnetization per spin greater than one. Instead ϵ^β is the density of all the spins in all the clusters in a volume ξ^d [11–13]. Because all of the clusters are identical, the density of each of these clusters is $\rho_c^{fc} \sim \epsilon^{1/2}/(R^d \epsilon^{2-d/2})$ at mean-field critical points and $\rho_s^{fc} \sim \Delta h^{1/2}/(R^d \Delta h^{3/2-d/4})$ at spinodals. These densities are good approximations in near-mean-field systems. We will refer to these clusters as *fundamental clusters*. These clusters are not the critical phenomena fluctuations, but are related to them [11,12,15].

Spinodals mark the boundary between the metastable and unstable states. In near-mean-field systems the spinodal is not a sharp singularity but becomes a smeared out region [16] associated with singularities in complex temperature and magnetic field space [17]. As the spinodal is approached so is the limit of metastability [12]. Hence, we would expect that nucleation events, which form another class of clusters, also play a role in the CA model. From the Langevin approach [5,6] we find that the nucleation clusters are local regions of growth of the stable high stress phase in the metastable low stress phase. An earthquake represents the stress release due to the decay of the high stress phase into the metastable low stress phase. Because the nucleation phenomena of interest occurs near the spinodal, the classical picture is not valid [18,19]. Instead, a calculation of the nucleation rate must include the effect of the spinodal which involves a vanishing of the surface tension [20]. With these considerations the nucleation rate, which is proportional to the number n of clusters per unit volume, is given by [20]

$$n \propto \frac{\Delta h^{1/2} \exp(-AR^d \Delta h^{3/2-d/4})}{R^d \xi^d}, \quad (1)$$

where A is a constant independent of R and Δh .

The nucleation rate in Eq. (1) contains an exponential term whose argument is the nucleation barrier. The static prefactor, which is independent of the dynamics of the model, is $1/\xi^d$, where $\xi = R\Delta h^{-1/4}$ is the correlation length near the spinodal [18,20,21]. The $\Delta h^{1/2}$ term is the kinetic prefactor and is dynamics specific [19,20]. For the CA model the distance from the spinodal is measured by the amount of stress dissipated, i.e., $\Delta h \sim K_L/K$ [22]. Finally, the extra factor of R^d in the denominator reflects the fact that the theory employs a coarse grained time scale [5], but our simulations use a time scale based on plate updates. Because the coarse graining time is proportional to the coarse graining volume R^d [23], this extra factor is included in the nucleation rate.

Our assumption is that the CA model behaves like an Ising model near the spinodal for mean-field and near-mean-field systems. In this limit [12–15], fundamental clusters and nucleation events, which involve coalescence of fundamental clusters [12], are the only clusters. Because it is the decay of the high stress clusters that is the “earthquakes” in this model, cluster scaling and earthquake scaling are the same. To understand how this point of view provides answers to the questions posed in the introduction we discuss the fundamental clusters.

In mean-field each block fails at the failure threshold and fails only once during an earthquake [5,6]. This behavior is an excellent approximation in near-mean-field [5]. The amount $\Delta\sigma$ of stress transmitted to a site during the failure of a cluster is proportional to the number of cluster sites in the interaction volume R^d , which is $\rho_s^{fc} R^d$ because we are near the spinodal, times the fraction of stress transmitted from a failed block, which is proportional to R^{-d} . Hence, $\Delta\sigma \sim \rho_s^{fc}$ during the failure of a fundamental cluster, and the mean size of the fundamental cluster is $s = \rho_s^{fc} \xi^d = \Delta h^{-1}$. The number of fundamental clusters per unit volume is $n_{fc} = R^d \Delta h^{3/2-d/4} / \xi^d = \Delta h^{3/2}$. Therefore, the density of fundamental clusters with s blocks scales as $n_{fc} \sim 1/s^{3/2}$.

To identify the fundamental clusters we examine the stresses on the blocks that make up a cluster of failed sites and determine the minimum stress, σ_{\min} , of the failing sites prior to failure, but after the update of the loader plate that triggers the event. We record *only* those events for which σ_{\min} is within the window $[\sigma^F - \Delta\sigma, \sigma^F]$. In Fig. 2 we plot the log of the number of fundamental clusters versus $\log s$. For the chosen parameters, $\Delta h = 0.01$ so that $\Delta\sigma \sim 0.01$. The slope of 1.53 is consistent with the theoretical prediction. The mean size $s = \Delta h^{-1} = 100$ is also consistent with our data. Note the lack of data spread. In Figs. 1 and 2 the fundamental clusters make up only the small s end of the scaling plot, but the fundamental clusters comprise $\sim 17 \times 10^6$ out of

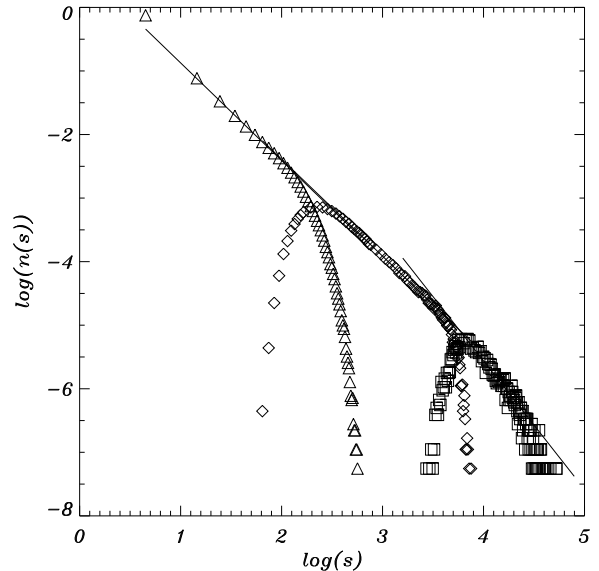


FIG. 2. Same data as Fig. 1, with the events separated into different classes. The triangles represent fundamental clusters with scaling exponent of 1.5 ± 0.05 . The diamonds are failing nucleation clusters with a scaling exponent 1.5 ± 0.05 , showing the absence of critical slowing down. The open squares are arrested nucleation events with a scaling exponent 2.0 ± 0.1 indicating the presence of critical slowing down. There are “breakout” events at the largest end of the plot that do not exhibit scaling.

18×10^6 events. Hence, a simulation of earthquake faults will require huge numbers of events to probe the statistics of the interesting and important large event region.

We now consider the nucleation events and their clusters. The size of the nucleation events depends on several factors that determine precisely when a given high stress nucleation event will stop growing. We will concentrate on two regimes. The first is events near the top of the saddle point hill associated with the barrier between the stable and metastable state [18,20]. The reason we neglect clusters on all scales between the fundamental clusters and the saddle point clusters is that Ising model studies have found no clusters in this intermediate region [12,15]. Another aspect of nucleation events of this kind in Ising systems is that one must get very close to the spinodal to observe critical slowing down because the saddle point hill appears to be high but not very flat until the system is very close to the spinodal [12,24]. The absence of critical slowing down near the saddle point also has been seen in the CA model [23]. Hence, there is a class of nucleation events that do not quite reach the top of the saddle point hill. As a result, random fluctuations lead to the decay of these clusters back to the metastable phase. We call these clusters *failing nucleation events*. The probability of these events is

characterized by a saddle point calculation without the kinetic prefactor. From these considerations and Eq. (1), the mean number of failing nucleation events per unit volume is $n_{\text{fn}} \propto \exp(-AR^d\Delta h^{3/2-d/4})/\xi^d$, the same as Eq. (1) without the kinetic prefactor.

To obtain predictions for the scaling regime two results are needed. The first is that $s_{\text{fn}} = \Delta h^{1/2}\xi^d$, where $\Delta h^{1/2}$ is the density of the nucleating cluster [20]. Second, because the exponential is a rapidly increasing function of its argument, as Δh decreases, the probability of a cluster increases from almost zero to a relatively large number over a very short interval of Δh . The value of Δh where this crossover occurs is the limit of metastability [16]. For this reason essentially all of the nucleation events take place at a fixed value of $AR^d\Delta h^{3/2-d/4} = C$. As for the fundamental clusters the stress transfer to a site in a nucleation event is equal to the density of the event. For our parameters the density is $\Delta h^{1/2} = 0.1$. Hence we identify these nucleating clusters by selecting *only* those events whose σ_{min} falls within the window [0.90, 0.99]. The size of the event is $s_{\text{fn}} = \Delta h^{1/2}\xi^d \sim 1000$ and the number of these events is $n_{\text{fn}} \propto e^C/\xi^d$. Using the relation between R and Δh implied by a fixed value of C , we find that n_{fn} scales as $1/s_{\text{fn}}^{3/2}$. In Fig. 2 we show a log-log plot of n_{fn} versus s_{fn} . The slope and mean size are consistent with our predictions.

Finally, we consider a second class of nucleation events. These are the events that have made it to the top and over the saddle point hill and have become arrested during their growth phase, i.e., after growing to some size the high stress nucleation region decays back to the low stress metastable state. Because the clusters have made it to the top of the saddle point hill, this decay of the high stress phase is no longer induced by random fluctuations: it appears in the Langevin approach due to a decreasing loader plate velocity on the coarse grained scale [5,22] which pulls the system away from the spinodal. We will call these clusters *arrested nucleation events*.

Because these clusters experience critical slowing down, their number per unit volume is given by Eq. (1). A key feature in the growth of nucleation events near the spinodal is that their initial growth is a filling in [24], and hence these clusters are compact, that is $s_{\text{an}} \propto \xi^d = R^d\Delta h^{-d/4}$. The density is of order unity so that we will identify these events with those clusters whose minimum stress of the failing blocks obeys the condition $\sigma_{\text{min}} < 0.90$. Using the same arguments as in for the failing nucleation events, we find that their mean size is about 10^4 and the slope of the scaling plot is predicted to be 2. The data presented in Fig. 2 is consistent with these predictions.

In summary, these theoretical considerations and numerical results strongly suggest several important points. (1) Earthquake fault models are statistically dominated by small, and in the case of real earthquakes, uninter-

esting events. (2) The large and small events have different physical mechanisms. (3) The scaling regime is composed of events with two different power law distributions, which accounts for the data spread at the large events end of the scaling plot in Fig. 1. (4) Note that there is still a spread in the data at the large events end of Fig. 2 and that these events do not scale with a slope of 2. Numerical investigation indicates that these are “breakout” events that are generated by the spatial coalescence of arrested nucleation events [26] and are beyond the assumptions of our present theoretical treatment. That is, as the arrested high stress cluster decays, it releases stress into the surrounding system. If, due to past history, the stress field is unstable, this stress release can lead to runaway failure. This type of event was considered in Ref. [25] and is a fourth mechanism that must be considered in the generation of earthquakes. In contrast, the nucleation events are generated by the coalescence of overlapping fundamental clusters occupying the same region of volume ξ^d .

We would like to acknowledge useful conversations with F. J. Alexander and H. Gould. The work of M. A. and W. K. was supported by DOE DE-FG02-95ER14498, and that of J. B. R. and J. S. S. M. by DOE DE-FG03-95ER14499. This work, LA-UR-00-0740, was also partially supported by the Department of Energy under contract W-7405.

-
- [1] B. Gutenberg and C. F. Richter, *Seismicity of the Earth and Associated Phenomena*, Princeton University Press, Princeton (1954).
 - [2] C. Scholz, *The Mechanics of Earthquakes and Faulting*, Cambridge University Press, Cambridge (1990).
 - [3] R. Burridge and L. Knopoff, *Bull. Seism. Soc. of Amer.* **57**, 341 (1967).
 - [4] J. M. Carlson and J. S. Langer, *Phys. Rev. A* **40**, 6470 (1989).
 - [5] C. D. Ferguson, W. Klein and J. B. Rundle, *Phys. Rev. E* **60**, 1359 (1999).
 - [6] W. Klein, J. B. Rundle and C. D. Ferguson, *Phys. Rev. Lett.* **78**, 3793 (1997).
 - [7] J. B. Rundle, W. Klein, S. Gross and D. Turcotte, *Phys. Rev. Lett.* **75**, 1658 (1995).
 - [8] S. K. Ma *Modern Theory of Critical Phenomena*, Benjamin, Reading, MA (1976).
 - [9] A. Coniglio and W. Klein, *J. Phys. A* **13**, 2775 (1980).
 - [10] W. Klein, *Phys. Rev. Lett.* **65**, 1462 (1990).
 - [11] W. Klein, H. Gould, J. Tobochnik, F. J. Alexander, M. Anghel, and G. Johnson, *cond-mat/0001230*.
 - [12] L. Monette and W. Klein, *Phys. Rev. Lett.* **68**, 2336 (1992).
 - [13] T. Ray and W. Klein, *J. Stat. Phys.* **53**, 773 (1988).
 - [14] T. Ray and W. Klein, *J. Stat. Phys.* **61**, 891 (1990).

- [15] F. J. Alexander and W. Klein (in preparation).
- [16] K. Binder, Phys. Rev. A **29**, 341 (1984).
- [17] H. Gould and W. Klein (in preparation).
- [18] J. S. Langer, Annals of Physics **41**, 108 (1967).
- [19] J. S. Langer, Annals of Physics **54**, 258 (1969).
- [20] C. Unger and W. Klein, Phys. Rev. B **29**, 2698 (1984).
- [21] J. Lee, M. A. Novotny and P. Rikvold, Phys. Rev. E **52**, 356 (1995).
- [22] W. Klein, M. Anghel, C. D. Ferguson, J. B. Rundle, and J. S. Sá Martins, American Geophysical Union Volume on the Physics of Earthquakes (accepted for publication).
- [23] C. D. Ferguson, Ph.D. Thesis, Boston University (1996).
- [24] D. W. Heermann and W. Klein, Phys. Rev. Lett. **50**, 1062 (1983).
- [25] J. B. Rundle, E. Preston, S. McGinnis, and W. Klein, Phys. Rev. Lett. **80**, 5698 (1998).
- [26] M. Anghel and W. Klein (in preparation).